

Received Date : 20-Sep-2016
Revised Date : 07-Dec-2016
Accepted Date : 09-Dec-2016
Article type : Original Article

The iron-sulfur cluster biosynthesis protein SUFB is required for chlorophyll synthesis, but not phytochrome signaling

Xueyun Hu^{1,2}, Mike T. Page³, Akihiro Sumida¹, Ayumi Tanaka¹, Matthew J. Terry^{3,4}, Ryouichi Tanaka^{1*}

¹Institute of Low Temperature Science, Hokkaido University, Sapporo 060-0819, Japan; ²School of Life Science and Engineering, Southwest University of Science and Technology, Mianyang City, Sichuan, 621010, China; ³Biological Sciences, University of Southampton, Southampton, UK; ⁴Institute for Life Sciences, University of Southampton, Southampton, UK.

*Corresponding Author: Ryouichi Tanaka, Institute of Low Temperature Science, Hokkaido University, N19W8 Kita-ku, Sapporo 060-0819, Japan; telephone and fax, +81-11-706-5494; e-mail, rtanaka@lowtem.hokudai.ac.jp

e-mail addresses of the other authors: Xueyun Hu, hy20030572@outlook.com; Mike T. Page, m.page2@lancaster.ac.uk; Akihiro Sumida, asumida@lowtem.hokudai.ac.jp; Ayumi Tanaka, ayumi@pop.lowtem.hokudai.ac.jp; Matthew J. Terry, mjt@soton.ac.uk

Running title: SUFB is required for chlorophyll synthesis

This article has been accepted for publication and undergone full peer review but has not been through the copyediting, typesetting, pagination and proofreading process, which may lead to differences between this version and the Version of Record. Please cite this article as doi: 10.1111/tpj.13455
This article is protected by copyright. All rights reserved.

Keywords: chloroplast, Fe-S cluster, chlorophyll biosynthesis, Mg-protoporphyrin monomethyl ester cyclase, far-red light, *Arabidopsis thaliana*

Summary

Proteins that contain iron-sulfur clusters play pivotal roles in various metabolic processes, such as photosynthesis and redox metabolism. Among the proteins involved in the biosynthesis of iron-sulfur clusters in plants, the SUFB subunit of the SUFBCD complex appears unique because SUFB has been reported to be involved in chlorophyll metabolism and phytochrome-mediated signaling. To gain insights into the function of the SUFB protein, we analyzed the phenotypes of two *SUFB* mutants, *laf6* and *hmc1*, and RNAi lines with reduced *SUFB* expression. When grown in the light, the *laf6* and *hmc1* mutants and the *SUFB* RNAi lines accumulated higher levels of the chlorophyll biosynthesis intermediate, Mg-protoporphyrin IX monomethylester (Mg-proto MME) consistent with the impairment of Mg-proto MME cyclase activity. Both SUFC- and SUFD-deficient RNAi lines accumulated the same intermediate suggesting that inhibition of Fe-S cluster synthesis is the primary cause of this impairment. Dark-grown *laf6* seedlings also showed an increase in protoporphyrin IX (Proto IX), Mg-proto, Mg-proto MME and 3,8-divinyl protochlorophyllide *a* (DV-Pchlde) levels, but this was not observed in *hmc1* or the *SUFB* RNAi lines, nor was it complemented by *SUFB* overexpression. In addition, the long hypocotyl in far-red light phenotype of the *laf6* mutant could not be rescued by *SUFB* overexpression and segregated from the pale-green SUFB-deficient phenotype indicating it is not caused by mutation at the *SUFB* locus. These results demonstrate that Fe-S cluster biosynthesis is important for chlorophyll biosynthesis, but that the *laf6* phenotype is not due to a *SUFB* mutation.

Introduction

Iron-sulfur (Fe-S) cluster cofactors play pivotal roles in various biological processes that are critical to life, such as photosynthesis and redox metabolism (Sheftel *et al.*, 2010; Balk and Pilon, 2011). In plastids, Fe-S proteins are involved in photosynthetic electron transport and nitrogen and sulfur assimilation and therefore Fe-S cluster biogenesis is essential for these processes. Several proteins have been shown to take part in the biogenesis of Fe-S clusters in plastids with the SUF system suggested to play a central role (Balk and Pilon, 2011). In an accompanying paper (Hu *et al.*, 2016), we provided *in planta* evidence that demonstrates the importance of the SUF system in general Fe-S cluster biosynthesis in plastids.

In the SUF system, the SUFB, SUFC and SUFD proteins form a complex, which is suggested to act as a scaffold to form Fe-S clusters. The Fe-S clusters are subsequently transferred to specific Fe-S carrier proteins before they are incorporated into Fe-S apoproteins (Balk and Pilon, 2011; Couturier *et al.*, 2013; Balk and Schaedler, 2014). This model is based on the mechanism revealed for the bacterial SUF proteins. In *Escherichia coli*, one SUFB, two SUFC and one SUFD protein form a SUFBC₂D complex that has been shown to function as a scaffold for Fe-S cluster assembly *in vitro* (Outten *et al.*, 2003; Chahal *et al.*, 2009; Wollers *et al.*, 2010). The protein sequences of plant SUFBs exhibit high similarity to their prokaryotic counterparts and *Arabidopsis* SUFB can complement SUFB deficiency in *E. coli* (Xu *et al.*, 2005). In addition, SUFB has been shown to interact with the evolutionary conserved plastidic SUFC protein (Xu *et al.*, 2005), which in turn can interact with *Arabidopsis* plastidic SUFD (Xu and Møller, 2004). Recently, we demonstrated that *Arabidopsis* SUFB, SUFC and SUFD form a protein complex like their bacterial counterparts indicating that the plant SUFBCD complex also functions as a scaffold for Fe-S cluster biosynthesis (Hu *et al.*, 2016). For better understanding of the roles of Fe-S cluster biosynthesis in plastids, various mutant plants in which Fe-S synthesizing activities are compromised have been analyzed. These mutants typically show a reduction in photosystem I

subunits that bind several Fe-S proteins as well as reduced levels of chlorophyll and a loss of accumulation of many photosynthetic proteins, including those without Fe-S clusters (Yabe *et al.*, 2004; Touraine *et al.*, 2004; Lezhneva *et al.*, 2004; Van Hoewyk *et al.*, 2007). However, the underlying reason for the reduced chlorophyll phenotypes is not currently established.

In higher plants, chlorophyll is synthesized from glutamate (Tanaka and Tanaka 2007; Mochizuki *et al.*, 2010; see Fig. S1). Three enzymatic steps synthesize 5-aminolevulinic acid (ALA) from glutamate and eight molecules of ALA are subsequently converted into protoporphyrinogen IX. Protoporphyrinogen IX is then oxidized by protoporphyrinogen IX oxidase to protoporphyrin IX (Proto IX), which is converted either into Mg-protoporphyrin IX (Mg-proto) by Mg-chelatase or into protoheme by ferrochelatase. This is the main branching point of chlorophyll biosynthesis. Mg-proto is further esterified to form Mg-proto monomethyl ester (Mg-proto MME). Conversion of Mg-proto MME to divinyl protochlorophyllide *a* (DV-Pchlde) by Mg-proto MME cyclase follows and Mg-proto MME is then modified to form monovinyl protochlorophyllide *a* (MV-Pchlde). Upon illumination, MV-Pchlde is reduced to chlorophyllide *a*, which is then esterified to form chlorophyll.

A number of *Arabidopsis* *SUF* mutants have been characterized to date and all show a pale green phenotype. This includes the *SUFB* mutant allele, *long after far-red 6 (laff6)*, which harbors a transposon insertion in the upstream untranslated region of the *SUFB* gene resulting in reduced *SUFB* expression (Møller *et al.*, 2001) and *hmc1* that has a base substitution in its coding sequence resulting in the replacement of a conserved proline with a leucine (Nagane *et al.*, 2010). Similarly, a *SUFD* T-DNA insertion mutant of *Arabidopsis* also showed a pale green phenotype with a reduced chlorophyll content (Hjorth *et al.*, 2005). These observations demonstrate that chlorophyll accumulation requires Fe-S cluster synthesis in *Arabidopsis* (Nagane *et al.*, 2010; Balk and Schaedler, 2014). In addition to a reduced chlorophyll accumulation, the two *SUFB* alleles mentioned above were both reported to

accumulate intermediates of chlorophyll metabolism: Proto IX for *laf6* (Møller *et al.*, 2001) and 7-hydroxymethyl-chlorophyll *a* and pheophorbide *a*, both of which are intermediates of chlorophyll breakdown, for *hmc1* (Nagane *et al.*, 2010). Since there was no report of mutants in other SUF proteins accumulating intermediates of chlorophyll metabolism, it was speculated that SUFB might play a specific role in the regulation of chlorophyll metabolism in addition to functioning in the biosynthesis of Fe-S clusters (Nagane *et al.*, 2010). SUFB has also been proposed to be involved in phytochrome signaling. The *laf6* mutant exhibited a long hypocotyl when seedlings were grown in far-red light suggesting that the *laf6* mutation affects phytochrome A signaling (Møller *et al.*, 2001). However, a long hypocotyl phenotype has not been reported for the other two *SUF* mutants and the role of SUFB in phytochrome signaling remains unclear.

Since it was reported that a knockout of *SUFB* was lethal at the embryonic stage (Nagane *et al.*, 2010), we have investigated the physiological roles of SUFB and Fe-S cluster biosynthesis by constructing conditional *SUFB* silencing lines using RNAi technology. In addition, we have expressed *SUFB* in the *laf6* mutant background to evaluate the effects of *SUFB* overexpression on its hypocotyl elongation phenotype. Through in depth analysis of these lines, we have been able to identify potential target sites of Fe-S cluster biosynthesis deficiency within the chlorophyll biosynthesis pathway, and clarified the hypotheses about the specific functions of SUFB in chlorophyll biosynthesis and phytochrome signaling.

Results

Depletion of SUFB by RNAi results in reduced chlorophyll levels

The two SUFB-deficient mutants characterized to date, *hmc1* and *laf6*, show rather different phenotypes with respect to chlorophyll biosynthesis and phytochrome responses. In the absence of available knock-out lines due to embryo lethality, we constructed conditional *SUFB*-silencing lines to further investigate the impact of *SUFB* depletion on these responses. In these lines, a dexamethasone (Dex)-inducible promoter drives the expression of artificial sequences that are complementary to part of the Arabidopsis *SUFB* gene leading to degradation of *SUFB* mRNA (see experimental procedures). It is possible that an RNAi construct suppresses some off-target gene expression and we therefore tested two independent RNAi constructs (*SUFB*-RNAi-1 and *SUFB*-RNAi-2) that were designed to interact with two different sequences within the *SUFB* gene. In agreement with previous SUFB-deficient lines, both *SUFB* RNAi lines showed a pale green phenotype in 4-week-old plants that was dependent on Dex treatment (Figure 1a). The pale phenotype of the *SUFB* RNAi lines correlated with the Dex-dependent loss of SUFB protein in these lines (Figure 1b). Analysis of chlorophyll levels showed that both RNAi lines were equally depleted in chlorophyll *a* and *b* and that the observed phenotype was stronger than seen for the *hmc1* mutant (Figure 1c), which shows a moderate reduction in chlorophyll levels in agreement with a previous report (Nagane *et al.* 2010). Identical results were obtained from 7 d-old mutant and *SUFB* RNAi seedlings grown on agar plates (Figure S2). Together, these results confirm that a reduction in SUFB leads to reduced chlorophyll accumulation.

The SUFBC₂D complex is required for chlorophyll synthesis

To determine how depletion of SUFB affects chlorophyll biosynthesis we measured the levels of key chlorophyll biosynthesis intermediates in the *hmc1* mutant and *SUFB* RNAi lines using high-performance liquid chromatography (Mochizuki *et al.*, 2008). As shown in Figure 2, Mg-proto MME accumulated in the *hmc1* mutant and the *SUFB* RNAi lines treated with Dex to levels in excess of WT lines. This was true both for mature plants (Figure 2a) and seedlings (Figure 2b). In contrast, all

SUFB-deficient lines had reduced levels of Proto IX, and showed reductions in Mg-proto (Figure S3).

These results indicate that Mg-proto MME cyclase activity is likely to be compromised in the *hmc1* mutant and the conditional *SUFB* RNAi lines as *Arabidopsis* mutants that are defective in Mg-proto MME cyclase activity accumulate this substrate (Tottey *et al.*, 2003; Peter *et al.*, 2009). As Mg-proto MME cyclase protein levels are unaltered in SUFB-deficient plants (Figure 2c) we conclude that this effect is at the level of Mg-proto MME cyclase activity. In addition, we interpret the lower levels of Proto IX and Mg-proto to be due to feedback inhibition in the tetrapyrrole pathway. A blockage in the cyclase step could result in more porphyrin directed towards heme leading to inhibition of ALA synthesis (Cornah *et al.*, 2003). It is also possible that oxidative stress effects are impairing tetrapyrrole biosynthesis via an alternative mechanism (Schlicke *et al.*, 2014).

The effect of SUFB deficiency could be due to an inhibition of Fe-S cluster synthesis or could be due to an independent function of the SUFB protein. To test this we analyzed the phenotype of conditional RNAi-silencing lines for *SUFD* and *SUFC* (Hu *et al.*, 2016). Both *SUFC* and *SUFD* RNAi lines showed pale-green leaves and were similar in appearance to *SUFB* lines (Figure 3a). In addition, in each case Mg-proto MME accumulated to a similar extent as observed for the *SUFB* RNAi line or *hmc1* (Figure 3b). These results therefore indicate that accumulation of Mg-proto MME is due to an impaired function of the SUFBC₂D complex and not to a unique function of SUFB.

Overexpression of SUFB complements the white-light grown phenotype of the *laf6* mutant

To determine whether all of the phenotypes observed in the *laf6* mutant allele were due to SUFB deficiency, we generated several independent transgenic lines that expressed 35S::*SUFB* in the *laf6* mutant, which is in the Landsberg *erecta* (*Ler*) background. Two overexpression lines (35S::*SUFB/laf6-4* and 7) were selected and used for further analysis (Figure 4a). The *laf6* mutant

shows a reduced level of the SUFB protein (to 15% of the WT (*Ler*) level), and this was increased in the two *SUFB* complemented lines, although the abundance of SUFB was still less than WT at 64% and 70% of the WT level, respectively (Figure 4b). Nevertheless, both 35S::*SUFB* lines restored the visibly pale phenotype of 4 week-old *laf6* plants to a WT appearance (Figure 4a) and this was confirmed by analysis of chlorophyll levels. As shown in Figure 4c, chlorophyll was significantly reduced in the *laf6* mutant in agreement with Møller *et al.* (2001), but both chlorophyll *a* and chlorophyll *b* levels were similar to wild-type in the 35S::*SUFB/laf6-4* and 7 lines. Identical results were observed in 7 d-old seedlings (Figure S4).

Next we examined the chlorophyll biosynthesis intermediates Proto IX, Mg-proto and Mg-proto MME. In agreement with what we observed in the *hmc1* mutant and SUFB RNAi lines (Figure 2), the *laf6* mutant also showed elevated levels of Mg-proto MME in 4 week-old plants (Figure 4d) and in seedlings (Figure 4e). This aspect of the *laf6* phenotype was fully complemented by overexpression of SUFB (Figure 4d, e). Similarly to other SUFB-deficient lines *laf6* also appeared to have slightly lower levels of Proto IX and Mg-proto, however this was not significant in this case (Figure S5).

Proto IX accumulation and long hypocotyl in far-red light phenotypes of *laf6* are not complemented by overexpression of SUFB

The *laf6* phenotype was originally characterized by an accumulation of Proto IX in dark- and far-red (FR) light-grown seedlings (Møller *et al.*, 2001). We therefore measured the levels of Proto IX and other chlorophyll precursors in 7 d-old WT and SUFB-deficient etiolated seedlings (Figure 5). First, we confirmed SUFB protein levels in dark-grown seedlings of all the lines used. As shown in Figure 5a, the *laf6* mutant contained reduced amounts of SUFB compared to WT (*Ler*) and the two complemented lines over-accumulated SUFB. Only a small decrease in SUFB was observed in *hmc1*, while in the

SUFB RNAi lines SUFB protein levels were severely reduced by Dex treatment. These results are consistent with those seen in 4 week-old plants (Figures 1b and 4b).

As reported by Møller *et al.* (2001), dark-grown *laf6* seedlings showed elevated levels of Proto IX compared to WT (*Ler*) seedlings (Figure 5b). In addition, Mg-proto, Mg-proto MME (Figure 5d, e) and 3,8-divinyl protochlorophyllide *a* (DV-Pchlide) (Figure 5f; Figure S6) all showed increased levels in *laf6* compared to WT (*Ler*). In contrast, neither the *hmc1* mutant or the *SUFB* RNAi lines showed elevated chlorophyll precursors in dark-grown seedlings (Figure 5c-f; Figure S6). In fact, *hmc1* and the *SUFB*-silenced etiolated seedlings accumulated less Proto IX than WT (*Col*) seedlings (Figure 5c). In addition, overexpression of *SUFB* did not rescue the increase in chlorophyll precursors seen in *laf6* (Figure 5b, d-f; Figure S6). Taken together, these results show that the excessive accumulation of Proto IX, Mg-proto, Mg-proto MME and DV-Pchlide in etiolated *laf6* seedlings is not the consequence of altered *SUFB* levels in this mutant.

The *laf6* mutant was originally isolated from a screen for mutants with a long hypocotyl after FR light (Møller *et al.*, 2001). To investigate this response and further explore the link between Fe-S cluster biosynthesis and phytochrome signaling, the response of the *SUFB* mutant and transgenic lines to FR light was examined. As expected, *laf6* had a longer hypocotyl than WT when grown under FR light irradiation (Figure 6a). However, this response was not rescued in the *SUFB*-complemented lines and the *SUFB* RNAi lines did not show enhanced hypocotyl elongation compared with WT (*Col*) seedlings on Dex (Figure 6a). These results show that the reduced responsiveness toward FR light in *laf6* is not correlated with *SUFB* levels in seedlings.

The long hypocotyl phenotype of *laf6* is due to a second, segregating mutation

The results in our hypocotyl elongation assays and on the accumulation of Proto IX and DV-Pchlde suggest that the *laf6* mutant has an additional mutation that causes that phenotype independently of its effect on SUFB protein levels. To examine this possibility, we analyzed the segregation of *laf6* phenotypes after backcrossing *laf6* with WT (*Ler*). Seedlings in the F₂ generation were analyzed initially for hypocotyl length in FR and subsequently for chlorophyll biosynthesis in white light (Figure 6b, c). F₂ seedlings segregated into two populations with longer (>5.5 mm) and shorter (<5.0 mm) hypocotyls. Of 234 seedlings measured, 176 seedlings (75.2%) had short hypocotyls while 58 seedlings (24.8%) had long hypocotyls, a ratio indicating that the hypocotyl length was controlled by a single recessive locus (Figure 6b). Twenty seedlings from the population with long hypocotyls were then grown under continuous white light and chlorophyll levels determined. Again two populations were observed with 12 (60%) showing higher chlorophyll levels (>2.5 mg/g FW) similar to the level seen in WT seedlings and 8 (40%) with lower chlorophyll levels (<2.0 mg/g FW) consistent with *laf6* seedlings (Figure 6c). These results indicate that the long hypocotyl phenotype under FR light and the low chlorophyll phenotype under white light are controlled by two independent genes. This is consistent with our data showing that the long hypocotyl phenotype is not due to SUFB deficiency.

The *laf6* mutant shows an accumulation of Proto IX and other chlorophyll precursors in dark-grown seedlings and we speculated that the long hypocotyl phenotype might be linked to a deficiency in synthesis of the phytochrome chromophore, phytochromobilin, which is synthesized from heme (Frankenberg-Dinkel and Terry, 2009; see Figure S1). This was initially examined using the chromophore analogue phycocyanobilin (PCB; Elich *et al.*, 1989) and it was concluded that *laf6* was not compromised in phytochrome chromophore synthesis (Møller *et al.*, 2001). However, it was subsequently shown that the altered chromophore structure of PCB cannot support a FR high irradiance response leading to inhibition of hypocotyl elongation (Hanzawa *et al.*, 2002), so we re-addressed this question by feeding the chromophore precursor biliverdin IX α . However, as shown in Figure S7,

biliverdin IX α did not rescue the long hypocotyl phenotype of *laf6*, but could rescue a *hy1* mutant control.

Discussion

Iron-sulfur clusters are required for chlorophyll synthesis

Mutants lacking SUFB are reduced in PSI subunit accumulation and have reduced chlorophyll levels (Hu *et al.*, 2016). However, it was unclear whether the reduction in chlorophyll was a consequence of a reduced accumulation of photosynthetic proteins or whether chlorophyll synthesis was directly affected.

Here we show that a reduction of SUFB protein levels results in excessive accumulation of the chlorophyll precursor Mg-proto MME and an overall reduction in chlorophyll levels. Both the *laf6* and *hmc1* SUFB-deficient mutant alleles showed this phenotype as did the *SUFB* RNAi knock-down lines. Moreover, the *SUFC* and *SUFD* RNAi lines both accumulated Mg-proto MME suggesting that all subunits of the SUFBC₂D complex are necessary for optimal chlorophyll synthesis and that an inhibition of Fe-S cluster biosynthesis is the critical factor. To date no chlorophyll *a* biosynthesis enzymes have been shown to be Fe-S proteins although two enzymes involved in chlorophyll metabolism, 7-hydroxymethyl-chlorophyll *a* reductase and pheophorbide *a* oxygenase, contain Fe-S clusters (Meguro *et al.*, 2011, Wang and Liu, 2016, Pruzinska *et al.*, 2003) and the substrates of both of these enzymes also accumulate in the *hmc1* mutant (Nagane *et al.*, 2010) (see Figure S1). It is also reported that siroheme biosynthesis requires an Fe-S protein, sirohydrochlorin ferrochelatase (Saha *et al.*, 2008), although the effect of Fe-S deficiency on siroheme biosynthesis is not clear at the present time.

Fe-S proteins, such as ferredoxin, could also be involved, but this has only been established for chlorophyll *a* oxygenase (Oster *et al.*, 2000) and heme oxygenase (Muramoto *et al.*, 2002). Mutants in both of these enzymes are pale in colour (Chory *et al.*, 1989, Espineda *et al.*, 1999; Terry, 1997) and thus

This article is protected by copyright. All rights reserved.

could be candidate targets for an impact of Fe-S cluster deficiency.

In the current study, we have demonstrated that Mg-proto MME accumulates in SUFB-deficient mutants. Accumulation of Mg-proto MME is seen in mutants that lack Mg-proto MME cyclase activity (Tottey *et al.*, 2003; Peter *et al.*, 2009; Hollingshead *et al.*, 2012) and we therefore propose that Mg-proto MME cyclase activity is impaired in the SUFB-deficient plants. Mg-proto MME cyclase is predicted to contain three subunits based on genetic and biochemical analysis in barley (Rzeznicka *et al.*, 2005), although only two, YCF54 and CLH27, have been identified (Albus *et al.*, 2012; Tottey *et al.*, 2003; Hollingshead *et al.*, 2012; Bollivar *et al.* 2012). However, neither of these subunits have Fe-S cluster-binding motifs (Tottey *et al.*, 2003; Hollingshead *et al.*, 2012). It is therefore possible that the third yet-unidentified cyclase subunit contains an Fe-S cluster. Alternatively, other Fe-S proteins may function to accept electrons from the cyclase, as the cyclase reaction requires an electron acceptor. We have previously observed that treatment of methylviologen, an inhibitor of photosystem I, causes accumulation of Mg-proto MME in cucumber seedlings (Aarti *et al.*, 2006). Therefore, it is possible that photosystem I, which contains three Fe-S clusters, is itself required for the cyclase reaction. Finally, it is possible that the regulation of Mg-proto MME cyclase is indirectly impaired in the SUFB-deficient plants. Little is known about the regulation of Mg-proto MME cyclase, except for the involvement of NADPH-dependent thioredoxin reductase C (NTRC). A mutant lacking this enzyme accumulates MgP-MME (Stenbaek *et al.*, 2008), thus it is possible that the SUFB-deficient plants analyzed in this study are also impaired in the redox network in which NTRC is involved.

The phenotype of *laf6* is partially due to second site mutations

When chlorophyll precursors were measured in dark-grown seedlings we observed differences between the *laf6* allele and other SUFB-deficient lines. The *hmc1* mutant and *SUFB* RNAi lines showed

moderate decreases in Proto IX, Mg-proto and Mg-proto MME, although this was not significant in all cases, and did not have reduced Pchlide levels. In contrast, the *laf6* mutant accumulated Proto IX, Mg-proto, Mg-proto MME and DV Pchlide *a* and showed a decrease in MV Pchlide *a* in dark-grown seedlings. The accumulation of Proto IX was consistent with a previous report (Møller *et al.*, 2001). It is difficult to explain this set of results, but one possibility is that the conversion of DV-Pchlide to MV-Pchlide is impaired in the *laf6* background and the general increase in porphyrins could be due to a regulatory effect such as product inhibition for enzymes prior to DV-Pchlide in the pathway. Importantly, with regard to the function of SUFB, the effect of the *laf6* mutation on porphyrin accumulation in dark-grown seedlings could not be rescued by overexpression of SUFB in contrast to the light-dependent phenotypes of *laf6*. These results therefore indicate that the increase in chlorophyll intermediates in dark-grown *laf6* seedlings is caused by a second site mutation in the *laf6* background.

In the original description of *laf6* the accumulation of Proto IX was linked to a long hypocotyl phenotype under FR light (Møller *et al.*, 2001). The authors had speculated that perturbations to tetrapyrrole synthesis might lead to an inhibition of phytochrome chromophore synthesis. We also tested this hypothesis, partly because more recent evidence indicated that the original control used could not have been successful (Hanzawa *et al.*, 2002), but saw no evidence that the long hypocotyl phenotype was caused by chromophore deficiency. None of the other SUFB-deficient lines tested had a long hypocotyl in FR light, and the phenotype was not complemented by SUFB expression. Moreover, segregation analysis following a backcross to WT seedlings demonstrated that the long hypocotyl phenotype of *laf6* was separable from the chlorophyll-deficient phenotype of SUFB-deficient plants, and therefore also due to a second site mutation. Whether the accumulation of porphyrins in dark-grown seedlings and the long hypocotyl phenotype in FR light are linked is not known. Both processes are phytochrome regulated (Whitelam *et al.*, 1993; McCormac and Terry, 2002), but while hypocotyl elongation is inhibited by phytochrome, porphyrin synthesis is promoted.

In conclusion, we have shown that deficiency in Fe-S cluster biosynthesis leads to reduced chlorophyll accumulation and have identified Mg-Proto MME cyclase activity as the most likely target of inhibition. This is the first step to understand the role of Fe-S cluster biosynthesis in chlorophyll metabolism and provides important clues about the mechanism of Mg-Proto MME cyclase. In addition, we have resolved the discrepancy between the phenotypes of different *SUFB* mutant alleles and demonstrated that the long hypocotyl phenotype of *laf6* is unrelated to deficiency in SUFB. Together, these results help clarify the role of Fe-S clusters in plant development.

Experimental procedures

Plant materials

The *Arabidopsis thaliana* *laf6* and *hmc1* mutants were described by Møller *et al.* (2001) and Nagane *et al.* (2010), respectively. Sterilised *Arabidopsis* seeds were sown on half-strength Murashige and Skoog (1/2 MS) medium containing 1% (w/v) sucrose and 0.8% (w/v) agar or soil. Seeds were kept in darkness at 4°C for 3 d to induce uniform germination. The plants were subsequently grown under long-day (16 h light/8h dark) growth conditions under fluorescent light (70-90 $\mu\text{mol m}^{-2} \text{s}^{-1}$ at 23°C). For pigment and immunoblotting analyses, either developing leaves of 4-week-old plants or the whole seedlings of 7-day-old plants were harvested. For experiments under FR light (6 $\mu\text{mol m}^{-2} \text{s}^{-1}$) and in the dark, seedlings were grown for 7d on 1/2 MS agar plates at 23°C.

For segregation experiments, surface sterilised seeds (*Ler*, *laf6*, *F₂₋₁* and *F₂₋₂*) were sown on 1/2MS in 1% (w/v) agar, pH 5.8. After a 3 d cold treatment (dark, 4 °C), seeds were transferred to WL (100 $\mu\text{mol m}^{-2} \text{s}^{-1}$, 23 °C) for 2 h, then incubated in the dark (23 °C) for 1 d. Seedlings were then grown for 6 d in FR light (23 °C). After the FR treatment, seedlings were gently flattened onto the medium surface and

photographed for hypocotyl length analysis. During this process, plates were kept in very low intensity WL light as much as possible. Twenty randomly selected seedlings displaying a long hypocotyl phenotype in FR light were then transferred to a separate plate. All seedlings were then supplemented with filter-sterilised 3% (w/v) sucrose and recovered in low intensity WL (4 d at 5 $\mu\text{mol m}^{-2} \text{s}^{-1}$ followed by 2 d at 25 $\mu\text{mol m}^{-2} \text{s}^{-1}$) before being transferred to WL (100 $\mu\text{mol m}^{-2} \text{s}^{-1}$) for 11 d. Chlorophyll assays were performed on five seedlings of each parent line, as well as the twenty randomly selected seedlings with long hypocotyls after the FR treatment.

Cloning and *Arabidopsis* transformation

For *laf6* complementation, a complementary DNA (cDNA) covering the coding region of *Arabidopsis SUFB* was cloned from *Arabidopsis* (Col ecotype) into pEarleyGate100 (Earley *et al.*, 2006) as it is described in our accompanying paper (Hu *et al.*, 2016). In brief, to generate dexamethasone (Dex)-inducible RNAi constructs, two 300-bp regions from the coding sequence of either *SUFB*, *SUFD* or *SUFC* were amplified by PCR using the primer sets described in our accompanying paper (Hu *et al.*, 2016). PCR products were cloned into the pENTR4 dual selection vector (Life Technologies), the resulting entry clones were recombined with the pOpOff2 (kan) vector (Wielopolska *et al.*, 2005) by LR Clonase II (Life Technologies) recombination reactions. All the construct was introduced into *Agrobacterium tumefaciens* strain GV3101 and used to infect *Arabidopsis* with the floral dip method (Clough and Bent, 1998). Two-week-old seedlings of transformants with the pEarleyGate100 vector were selected by spraying with BASTA and transformants containing the pOpOff2 (kan) vector were selected on 50 μM kanamycin on 1/2 MS plates. Third generation homozygous plants were employed for further analysis.

SUFB, *SUFC* and *SUFD* RNAi induction

Dex was first dissolved in ethanol to a concentration of 20 mM, and then diluted using 0.02% tween-20

aqueous solution to give a final concentration of 10 μM . To induce RNAi-mediated gene silencing, 3-week-old plants grown in soil were sprayed with 10 μM Dex solution. In control experiments, plants were sprayed with the aqueous solution without Dex, but containing the same concentration of ethanol and Tween-20. To induce *SUFB*-silencing in plants grown on 1/2 MS medium, ethanol with or without Dex, was added to autoclaved 1/2 MS medium (at about 55°C) to a final concentration of 10 μM . It is noted that the effects of RNAi suppression were only visible in developing leaves in mature 3 or 4-week-old plants. Therefore, only developing leaves were harvested for protein and pigment analyses.

Pigments analysis

For the segregation analysis, leaf tissue was weighed, and then extracted in ice-cold 80% acetone. Samples were centrifuged at 16,100 $\times g$ for 5 min, and the absorbance of the supernatant was determined at 647 nm and 663 nm using a U-2001 spectrophotometer (Hitachi, Tokyo). Total chlorophyll content ($\mu\text{g ml}^{-1}$) was calculated by combining the chlorophyll *a* ($12.25 A_{663} - 2.79 A_{647}$) and chlorophyll *b* ($21.5 A_{647} - 5.1 A_{663}$) values, before conversion to mg g^{-1} FW. For other experiments, chlorophyll and its intermediates were extracted from leaf tissue by homogenization with acetone, which was pre-cooled at -30°C to suppress endogenous chlorophyllase activity (Hu *et al.*, 2013). Extracts were subsequently centrifuged for 5 min at 20,000 $\times g$ at 4°C, and the supernatant was analyzed by HPLC using a symmetry C8 column (150 mm in length, 4.6 mm in I.D.; Waters, Milford, MA, USA) according to the method of Zapata *et al.* (2000). Chlorophyll concentrations were estimated from the absorption monitored at 410 nm. Chlorophyll *a* and *b* standards were purchased from Juntec Co. Ltd., Odawara, Japan and pheophorbide *a* was purchased from Wako Pure Chemical Industries, Ltd. Japan. A fluorescence detector (Hitachi, Tokyo, Japan) was used for the detection of Proto IX, Mg-Proto IX, Mg-Proto IX MME, DV-Pchlid *a* and MV-Pchlid *a* after separation by HPLC. Proto IX was detected at 634 nm following excitation at 400 nm; and Mg-Proto IX and Mg-Proto IX MME, were detected at

600 nm after excitation at 417 nm, while DV-Pchlide *a* and MV-Pchlide *a* were quantified by measuring absorbance at 439 nm.

Immunoblot analysis

Total protein was extracted from leaves using 10 volumes (v/w) of protein extraction buffer containing 50 mM Tris-HCl (pH 8.0), 12% (w/v) sucrose (Suc), 2% (w/v) lithium lauryl sulfate, and 1.5% (w/v) dithiothreitol. The protein concentration of samples was determined using the Rc-Dc protein assay kit (BioRad). Before SDS-PAGE separation, all samples were mixed with an equal volume of 2 x urea buffer containing 10 mM Tris-HCl (pH 8.0), 10% (w/v) Suc, 2% (w/v) SDS, 1 mM EDTA, 4 mM dithiothreitol, 0.04% (w/v) bromophenol blue and 10 M urea. Samples were then separated on a 14% polyacrylamide gel and electro-blotted to PVDF membranes. SUFB protein was detected using an anti-SUFB antiserum raised against recombinant *Arabidopsis* SUFB protein expressed in *E. coli* (Rosetta DE3, Merck). The antibody raised against *Arabidopsis* CHL27 was a kind gift from Prof. Sabeeha Merchant (University of California, Los Angeles, USA).

Statistical analysis

Samples from two ecotypes (*Ler* and *Col*) were analyzed separately. WT, mutants and the transgenic lines in each ecotype were first analyzed as explanatory variables by generalized linear mixed-effects models (GLMMs). Two *SUFB*-complementation lines (35S::*SUFB/laf6*-4 and 7) and two conditional *SUFB*-RNAi lines (*SUFB*-RNAi-1-12 and 2-2) in Figs. 2b, 3, 4, S2 and S4 were nested and treated as random effects variables. After confirming significance of GLMMs ($p < 0.05$), multiple pairwise comparison was made with the Tukey Contrasts Fit for each result by using the "glht()" function of the "multicomp" package (Hothorn *et al.*, 2008) of R (ver. 3.2.2; R Core Team, 2015), which allows

Accepted Article

simultaneous tests for mixed-effects models outputs.

Acknowledgements

We thank Ms. Junko Kishimoto for her help in drawing figures and to Mr. Daniel Trim for performing the phytochrome chromophore feeding experiment. We are grateful to Professor Sabeeha Merchant (University of California, Los Angeles) for her kind gift of anti-Mg-Proto IX MME cyclase antiserum and to Professor Simon Møller (University of Stavanger, Norway; currently St. John's University, New York, USA) for *laf6* mutant seeds. This work was supported by Biotechnology and Biological Sciences Research Council grant BB/J018139/1 to MJT, by the CREST program, Japan Science and Technology Agency to AT, and by JSPS KAKENHI Grant Number 16H0655416 to RT. The authors declare no conflict of interest.

Short Supporting Information Legends

Additional Supporting information may be found in the online version of this article.

Figure S1. Tetrapyrrole biosynthetic pathway.

Figure S2. Phenotype of 7-day-old SUFB-deficient seedlings grown on 1/2 MS medium under long-day conditions.

Figure S3. Analysis of chlorophyll biosynthetic intermediates in SUFB-deficient plants.

Figure S4. Complementation of *laf6* with *SUFB*.

Figure S5. Proto IX (a) and Mg-proto (b) content of the developing leaves of 4-week-old *laf6* and *SUFB* overexpressing lines in a *laf6* background grown on soil under long-day conditions.

Figure S6. Detection of Pchlide *a* in 7-day-old etiolated mutant and transgenic seedlings with altered *SUFB* levels.

Figure S7. The effects of 0.1mM biliverdin IX α (BV) on hypocotyl length under far-red light of 6d-old WT, *laf6*, *hy1* and *phyA* seedlings.

References

Aarti, P.D., Tanaka, R. and Tanaka, A. (2006) Effects of oxidative stress on chlorophyll biosynthesis in cucumber (*Cucumis sativus*) cotyledons. *Physiol Plant*, **128**, 186–197.

Albus, C.A., Salinas, A., Czarnecki, O., et al. (2012) LCAA , a novel factor required for magnesium protoporphyrin monomethylester cyclase accumulation and feedback control of aminolevulinic acid. *Plant Physiol.*, **160**, 1923–1939.

Balk, J. and Pilon, M. (2011) Ancient and essential: the assembly of iron-sulfur clusters in plants. *Trends Plant Sci.*, **16**, 218–226.

Balk, J. and Schaedler, T.A. (2014) Iron cofactor assembly in plants. *Annu. Rev. Plant Biol.*, **65**,

Bollivar, D., Braumann, I., Berendt, K., Gough, S.P. and Hansson, M. (2014) The Ycf54 protein is part of the membrane component of Mg-protoporphyrin IX monomethyl ester cyclase from barley (*Hordeum vulgare* L.). *FEBS J.*, **281**, 2377–2386.

Chahal, H. K., Dai, Y., Saini, A., Ayala-Castro, C., and Outten, F. W. (2009) The SufBCD Fe-S scaffold complex interacts with SufA for Fe-S cluster transfer. *Biochemistry*, **48**, 10644–10653.

Chory, J., Peto, C.A., Ashbaugh, M., Saganich, R., Pratt, L. and Ausubel, F. (1989) Different Roles for Phytochrome in Etiolated and Green Plants Deduced from Characterization of *Arabidopsis thaliana* Mutants. *Plant Cell*, **1**, 867–880.

Clough, S.J. and Bent, A.F. (1998) Floral dip: a simplified method for *Agrobacterium*-mediated transformation of *Arabidopsis thaliana*. *Plant J.*, **16**, 735–743.

Cornah, J.E., Terry, M.J. and Smith, A.G. (2003) Green or red: what stops the traffic in the tetrapyrrole pathway? *Trends Plant Sci.*, **8**, 224–230.

Couturier, J., Touraine, B., Briat, J.-F., Gaymard, F. and Rouhier, N. (2013) The iron-sulfur cluster assembly machineries in plants: current knowledge and open questions. *Front. Plant Sci.*, **4**, e259.

Earley, K.W., Haag, J.R., Pontes, O., Opper, K., Juehne, T., Song, K. and Pikaard, C.S. (2006) Gateway-compatible vectors for plant functional genomics and proteomics. *Plant J.*, **45**, 616–629.

Elich, T.D., McDonagh, A.F., Palma, L.A. and Lagarias, J.C. (1989) Phytochrome Chromophore Biosynthesis. *J. Biol. Chem.*, **264**, 183–189.

Espineda, C.E., Linford, A.S., Devine, D. and Brusslan, J.A. (1999) The AtCAO gene, encoding

chlorophyll a oxygenase, is required for chlorophyll b synthesis in *Arabidopsis thaliana*. *Proc. Natl. Acad. Sci. U. S. A.*, **96**, 10507–10511.

Frankenberg-Dinkel, N. and Terry, M.J. (2009) Synthesis and role of bilins in photosynthetic

organisms. In *Tetrapyrroles: Birth, Life and Death* (Martin J. Warren, M.J. and Smith, A.G., eds.) New York: Springer, pp. 208-220.

Hanzawa, H., Shinomura, T., Inomata, K., Kakiuchi, T., Kinoshita, H., Wada, K. and Furuya, M.

(2002) Structural requirement of bilin chromophore for the photosensory specificity of phytochromes A and B. *Proc. Natl. Acad. Sci. U. S. A.*, **99**, 4725–4729.

Hjorth, E., Hadfi, K., Zauner, S. and Maier, U.G. (2005) Unique genetic compartmentalization of the

SUF system in cryptophytes and characterization of a SufD mutant in *Arabidopsis thaliana*. *FEBS Lett.*, **579**, 1129–1135.

Hollingshead, S., Kopečá, J., Jackson, P.J., Canniffe, D.P., Davison, P.A., Dickman, M.J., Sobotkas, R. and Hunter, C.N. (2012) Conserved chloroplast open-reading frame *ycf54* is required for

activity of the magnesium protoporphyrin monomethylester oxidative cyclase in *synechocystis* PCC 6803. *J. Biol. Chem.*, **287**, 27823–27833.

Hothorn, T., Bretz, F., Westfall, P. and Heiberger, R.M. (2008) Simultaneous inference in general

parametric models. *Biometrical J.*, **50**, 346–363.

Hu, X., Kato, Y., Tanaka, A. and Tanaka, R. (2016) The SUFBC₂D complex is required for the

biogenesis of all major classes of plastid Fe-S protein. *Plant J.* (submitted).

Hu, X., Tanaka, A. and Tanaka, R. (2013) Simple extraction methods that prevent the artifactual conversion of chlorophyll to chlorophyllide during pigment isolation from leaf samples. *Plant Methods*, **9**, e19.

Lezhneva, L., Amann, K. and Meurer, J. (2004) The universally conserved HCF101 protein is involved in assembly of [4Fe-4S]-cluster-containing complexes in *Arabidopsis thaliana* chloroplasts. *Plant J.*, **37**, 174–185.

McCormac, A.C. and Terry, M.J. (2002) Light-signalling pathways leading to the co-ordinated expression of HEMA1 and Lhcb during chloroplast development in *Arabidopsis thaliana*. *Plant J.*, **32**, 549–559.

Meguro, M., Ito, H., Takabayashi, A., Tanaka, R. and Tanaka, A. (2011) Identification of the 7-hydroxymethyl chlorophyll a reductase of the chlorophyll cycle in *Arabidopsis*. *Plant Cell*, **23**, 3442–3453.

Mochizuki, N., Tanaka, R., Grimm, B., Masuda, T., Moulin, M., Smith, A.G., Tanaka, A. and Terry, M.J. (2010) The cell biology of tetrapyrroles: A life and death struggle. *Trends Plant Sci.*, **15**, 488–498.

Mochizuki, N., Tanaka, R., Tanaka, A., Masuda, T. and Nagatani, A. (2008) The steady-state level of Mg-protoporphyrin IX is not a determinant of plastid-to-nucleus signaling in *Arabidopsis*. *Proc. Natl. Acad. Sci. U. S. A.*, **105**, 15184–15189.

Møller, S.G., Kunkel, T. and Chua, N.H. (2001) A plastidic ABC protein involved in intercompartmental communication of light signaling. *Genes Dev.*, **15**, 90–103.

Muramoto, T., Tsurui, N., Terry, M.J., Yokota, A. and Kohchi, T. (2002) Expression and biochemical properties of a ferredoxin-dependent heme oxygenase required for phytochrome chromophore synthesis. *Plant Physiol.*, **130**, 1958–1966.

Nagane, T., Tanaka, A. and Tanaka, R. (2010) Involvement of AtNAP1 in the regulation of chlorophyll degradation in *Arabidopsis thaliana*. *Planta*, **231**, 939–949.

Oster, U., Tanaka, R., Tanaka, A. and Rüdiger, W. (2000) Cloning and functional expression of the gene encoding the key enzyme for chlorophyll b biosynthesis (CAO) from *Arabidopsis thaliana*. *Plant J.*, **21**, 305–310.

Outten, F. W., Wood, M. J., Munoz, F. M., and Storz, G. (2003) The SufE protein and the SufBCD complex enhance SufS cysteine desulfurase activity as part of a sulfur transfer pathway for Fe-S cluster assembly in *Escherichia coli*. *J Biol Chem* **278**, 45713–45719.

Peter, E., Salinas, A., Wallner, T., Jeske, D., Dienst, D., Wilde, A. and Grimm, B. (2009) Differential requirement of two homologous proteins encoded by *sll1214* and *sll1874* for the reaction of Mg protoporphyrin monomethylester oxidative cyclase under aerobic and micro-oxic growth conditions. *Biochim. Biophys. Acta - Bioenerg.*, **1787**, 1458–1467.

Pruzinská, A., Tanner, G., Anders, I., Roca, M. and Hörtensteiner, S. (2003) Chlorophyll breakdown: pheophorbide a oxygenase is a Rieske-type iron-sulfur protein, encoded by the accelerated cell death 1 gene. *Proc. Natl. Acad. Sci. U. S. A.*, **100**, 15259–15264.

R Core Team (2015). R: A language and environment for statistical computing. R Foundation for Statistical Computing, Vienna, Austria. URL <https://www.R-project.org/>.

Rzeznicka, K., Walker, C.J., Westergren, T., Kannangara, C.G., Wettstein, D. von, Merchant, S.,

Gough, S.P. and Hansson, M. (2005) Xantha-l encodes a membrane subunit of the aerobic Mg-protoporphyrin IX monomethyl ester cyclase involved in chlorophyll biosynthesis. *Proc. Natl. Acad. Sci. U. S. A.*, **102**, 5886–5891.

Saha, K., Webb, M. E., Rigby, S. E. J., Leech, H. K., Warren, M. J. and Smith, A. G. (2012) Characterization of the evolutionarily conserved iron–sulfur cluster of sirohydrochlorin ferrochelatase from *Arabidopsis thaliana*. *Biochem. J.*, **444**, 227–237.

Schlicke, H., Salinas, A., Firtzlaff, V., Richter, A.S., Glässer, C. and Maier, K. (2014) Induced Deactivation of Genes Encoding Chlorophyll Biosynthesis Enzymes Disentangles Tetrapyrrole-Mediated Retrograde Signaling. *Mol. Plant*, **7**, 1211–1227.

Sheftel, A., Stehling, O. and Lill, R. (2010) Iron-sulfur proteins in health and disease. *Trends Endocrinol. Metab.*, **21**, 302–314.

Stenbaek, A., Hansson, A., Wulff, R. P., Hansson, M., Dietz, K.-J., and Jensen, P. E. (2008) NADPH-dependent thioredoxin reductase and 2-Cys peroxiredoxins are needed for the protection of Mg-protoporphyrin monomethyl ester cyclase. *FEBS Letters*, **582**, 2773–2778.

Tanaka, R. and Tanaka, A. (2007) Tetrapyrrole biosynthesis in higher plants. *Annu. Rev. Plant Biol.*, **58**, 321–346.

Terry, M.J. (1997) Phytochrome chromophore-deficient mutants. *Plant Cell Environ.*, **20**, 740–745.

Tottey, S., Block, M.A., Allen, M., Westergren, T., Albrieux, C., Scheller, H. V, Merchant, S. and Jensen, P.E. (2003) *Arabidopsis* CHL27, located in both envelope and thylakoid membranes, is required for the synthesis of protochlorophyllide. *Proc. Natl. Acad. Sci. U. S. A.*, **100**, 16119–16124.

Touraine, B., Boutin, J.P., Marion-Poll, A., Briat, J.F., Peltier, G. and Lobréaux, S. (2004) Nfu2: A

scaffold protein required for [4Fe-4S] and ferredoxin iron-sulphur cluster assembly in *Arabidopsis* chloroplasts. *Plant J.*, **40**, 101–111.

Wang, X. and Liu, L. (2016) Crystal Structure and Catalytic Mechanism of 7-Hydroxymethyl Chlorophyll a Reductase. *J. Biol. Chem.*, **291**, 13349–13359.

Whitelam, G.C., Johnson, E., Peng, J., Carol, P., Anderson, M.L., Cowl, J.S. and Harberd, N.P. (1993) Phytochrome A null mutants of *Arabidopsis* display a wild-type phenotype in white light. *Plant Cell*, **5**, 757–768.

Wielopolska, A., Townley, H., Moore, I., Waterhouse, P. and Helliwell, C. (2005) A high-throughput inducible RNAi vector for plants. *Plant Biotechnol. J.*, **3**, 583–590.

Wollers, S., Layer, G., Garcia-Serres, R., Signor, L., Clemancey, M., Latour, J.-M., Fontecave, M. and Ollagnier de Choudens, S. (2010) Iron-sulfur (Fe-S) cluster assembly: the SufBCD complex is a new type of Fe-S scaffold with a flavin redox cofactor. *J. Biol. Chem.*, **285**, 23331–23341.

Xu, X.M., Adams, S., Chua, N. and Møller, S.G. (2005) AtNAP1 represents an atypical SufB protein in *Arabidopsis* plastids. *J. Biol. Chem.*, **280**, 6648–6654.

Xu, X.M. and Møller, S.G. (2004) AtNAP7 is a plastidic SufC-like ATP-binding cassette ATPase essential for *Arabidopsis* embryogenesis. *Proc. Natl. Acad. Sci. U. S. A.*, **101**, 9143–9148.

Yabe, T., Morimoto, K., Kikuchi, S., Nishio, K., Terashima, I. and Nakai, M. (2004) The *Arabidopsis* chloroplastic NifU-like protein CnfU, which can act as an iron-sulfur cluster scaffold

protein, is required for biogenesis of ferredoxin and photosystem I. *Plant Cell*, **16**, 993–1007.

Zapata, M., Rodríguez, F. and Garrido, J.L. (2000) Separation of chlorophylls and carotenoids from marine phytoplankton, a new HPLC method using a reversed phase C8 column and phridine-containing mobile phases. *Mar. Ecol. Prog. Ser.*, **195**, 29–45.

Accepted Article

Figure legends

Figure 1. Phenotype of 4-week-old SUFB-deficient plants grown on soil under long-day conditions. Conditional *SUFB*-silenced lines (*SUFB*-RNAi-1-12 and 2-2) were analysed with and without 10 µM dexamethasone (Dex) together with the SUFB-deficient *hmc1* mutant. (a) Phenotype of SUFB-deficient plants. (b) SUFB protein levels in SUFB-deficient mutant and transgenic lines. Total protein extracts (8 µg protein) of developing leaves were analyzed by immunoblotting using anti-SUFB antiserum (upper row) and the membrane was subsequently stained by Coomassie brilliant blue (CBB) as a loading control (bottom row). (c) Chlorophyll *a* and *b* content of developing leaves of SUFB-deficient plants. Data points represent the mean ± SD of four biological replicates. Letters in black (chlorophyll *a*) or in grey (chlorophyll *b*) above each bar indicate significant differences ($P < 0.05$) by Tukey's multiple-comparison test.

Figure 2. Analysis of chlorophyll biosynthetic intermediates in SUFB-deficient plants. Conditional SUFB-silenced lines (*SUFB*-RNAi-1-12 and 2-2) were analysed with and without 10 µM dexamethasone (Dex) together with the SUFB-deficient *hmc1* mutant. Mg-proto MME content in (a) developing leaves of 4-week-old plants grown on soil under long-day conditions or (b) in 7-day-old seedlings grown on 1/2 MS medium under long-day conditions. Data points represent the mean ± SD of

four biological replicates. Letters above each bar indicate significant differences ($P < 0.05$) by Tukey's multiple-comparison test. (c) The abundance of Mg-Proto IX cyclase (CHL27) in SUFB-deficient mutant and transgenic lines. Total protein extracts (8 μ g protein) of developing leaves of 4-week-old plants grown on soil under long day conditions were analysed by immunoblotting using anti-CHL27 antisera. Anti-Rubisco large subunit (RbcL) antisera were used to detect RbcL as the loading control.

Figure 3. The phenotype of *SUFB*-, *SUFC*- and *SUFD*-deficient plants. Conditional *SUFB*-, *SUFC*-, and *SUFD*-silenced lines were analyzed after 10 μ M dexamethasone (Dex) treatment together with the SUFB-deficient *hmc1* mutant. (a) Phenotype of 4-week-old WT and transgenic plants 7 days after Dex treatment. (b) HPLC profiles of pigments extracted by acetone from young leaves of WT and transgenic plants after Dex treatment. The X axis indicates retention time. The Y axis indicates fluorescence intensity at 600 nm which was excited at 415 nm in arbitrary units.

Figure 4. Complementation of *laf6* with *SUFB*. (a) Comparison of *laf6* and *SUFB* overexpressing lines in a *laf6* background grown on soil for 3 weeks under long day conditions. (b) SUFB protein levels in the mutant and transgenic lines. Total protein extracts (8 μ g protein) of developing leaves were analyzed by immunoblotting using anti-SUFB antiserum (upper row) and the membrane was subsequently stained by Coomassie brilliant blue (CBB) as a loading control (bottom row). (c) Chlorophyll *a* and *b* content of developing leaves of mutant and transgenic plants. (d) Mg-proto MME content in developing leaves of 4-week-old plants grown on soil under long-day conditions. (e) Mg-proto MME content in 7-day-old seedlings grown on 1/2 MS medium under long-day conditions. Data points represent the mean \pm SD of four biological replicates. Letters in black or grey above each bar indicate significant differences ($P < 0.05$) by Tukey's multiple-comparison test.

Figure 5. The phenotype of dark-grown SUFB-deficient seedlings. Comparison of 7-day-old etiolated

seedlings of conditional SUFB-silenced lines, *hmc1*, *laf6* and *laf6* complemented lines expressing SUFB grown on 1/2 MS medium with 0.8% agar and 1% sucrose. (a) SUFB protein levels in mutant and transgenic seedlings. Total protein extracts (16 µg protein) were analyzed by immunoblotting using anti-SUFB antiserum (upper row) and the membrane was subsequently stained by Coomassie blue staining as a loading control (lower row). (b), (c) Proto IX contents in etiolated seedlings in the *Ler* (b) and *Col* (c) backgrounds. Data points represent the mean ± SD of three biological replicates. Letters above each bar indicate significant differences ($P < 0.05$) by Tukey's multiple-comparison test. (d) Mg-proto IX and (e) Mg-proto IX-MME contents of mutant and transgenic seedlings. Data points represent the mean ± SD of three biological replicates. Letters in black (MgP) or in grey (MgP-MME) above each bar indicate significant differences ($P < 0.05$) by Tukey's multiple-comparison test. (f) DV- or MV-Pchlida a contents in mutant and transgenic seedlings. Data points represent the mean ± SD of four biological replicates. Letters in black (DV-Pchlida a) or in grey (MV-Pchlida a) above each bar indicate significant differences ($P < 0.05$) by Tukey's multiple-comparison test. Proto IX, protoporphyrin IX; MgP, Mg-protoporphyrin IX; MgP-MME, MgP monomethyl ester; DV-Pchlida a, 3,8-divinyl protochlorophylide a; MV-Pchlida a, monovinyl protochlorophylide a.

Figure 6. Segregation of the *laf6* long-hypocotyl phenotype. (a) Hypocotyl length of *laf6*, *laf6* expressing *SUFB* and conditional *SUFB*-deficient seedling grown for 6 d under far-red (FR) light. Data shown are mean ± SD of four biological replicates. (b) and (c) Segregation of the long hypocotyl and pale leaf phenotypes of back-crossed *laf6* seedlings. (b) Histogram of hypocotyl lengths of *Ler*, *laf6* and *F₂* generation (*Ler* x *laf6*) seedlings after 6 d growth in FR. (c) Histogram of the foliar chlorophyll content of the parent lines and 20 randomly selected *F₂* seedlings with long hypocotyls after 6 d FR. Following the FR treatment, all seedlings were supplemented with 3% sucrose and recovered in low intensity white light (WL) (4 d at 5 µmol m⁻² s⁻¹ followed by 2 d at 25 µmol m⁻² s⁻¹) before being transferred to WL (100 µmol m⁻² s⁻¹) for 11 d.

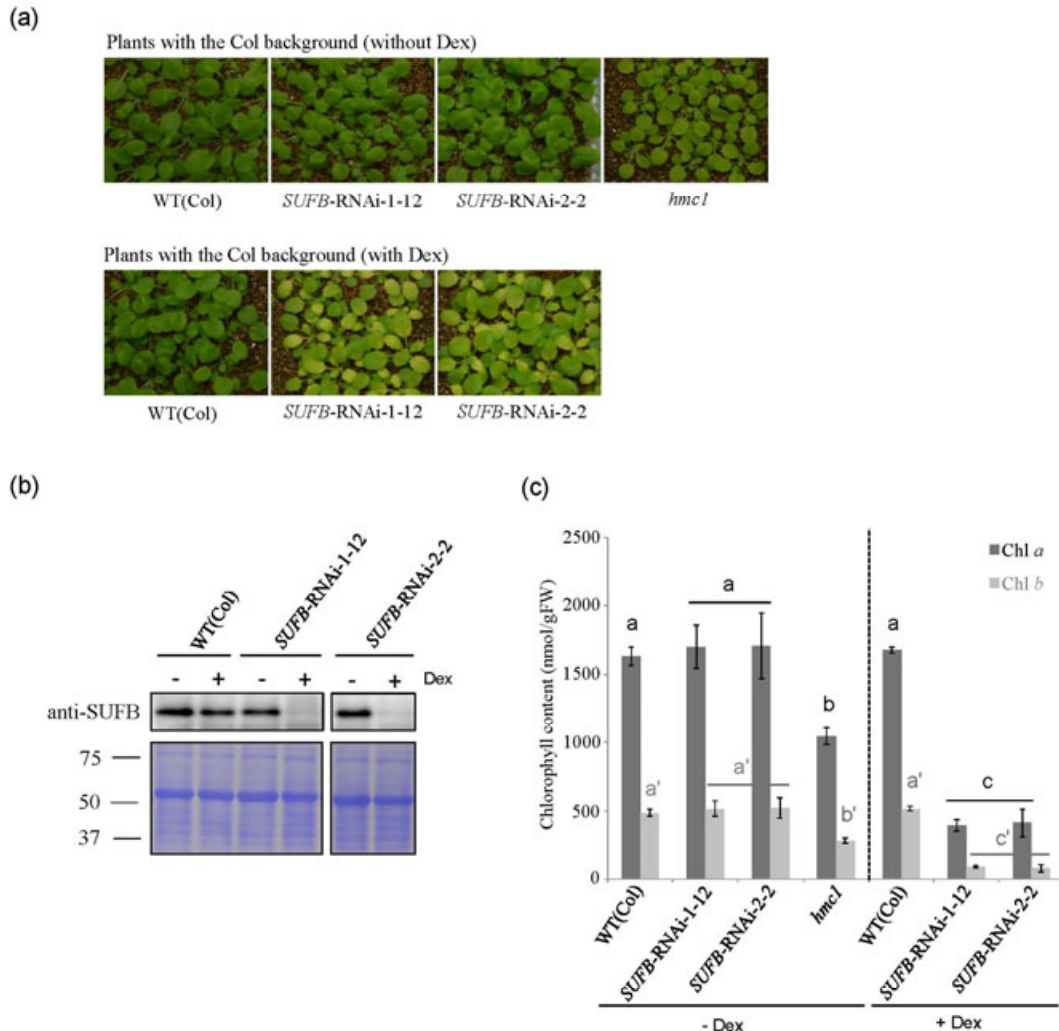


Figure 1. Phenotype of 4-week-old SUFB-deficient plants grown on soil under long-day conditions. Conditional SUFB-silenced lines (SUFB-RNAi-1-12 and 2-2) were analysed with and without 10 μ M dexamethasone (Dex) together with the SUFB-deficient *hmc1* mutant. (a) Phenotype of SUFB-deficient plants. (b) SUFB protein levels in SUFB-deficient mutant and transgenic lines. Total protein extracts (8 μ g protein) of developing leaves were analyzed by immunoblotting using anti-SUFB antiserum (upper row) and the membrane was subsequently stained by Coomassie brilliant blue (CBB) as a loading control (bottom row). (c) Chlorophyll a and b content of developing leaves of SUFB-deficient plants. Data points represent the mean \pm SD of four biological replicates. Letters in black (chlorophyll a) or in grey (chlorophyll b) above each bar indicate significant differences ($P < 0.05$) by Tukey's multiple-comparison test.

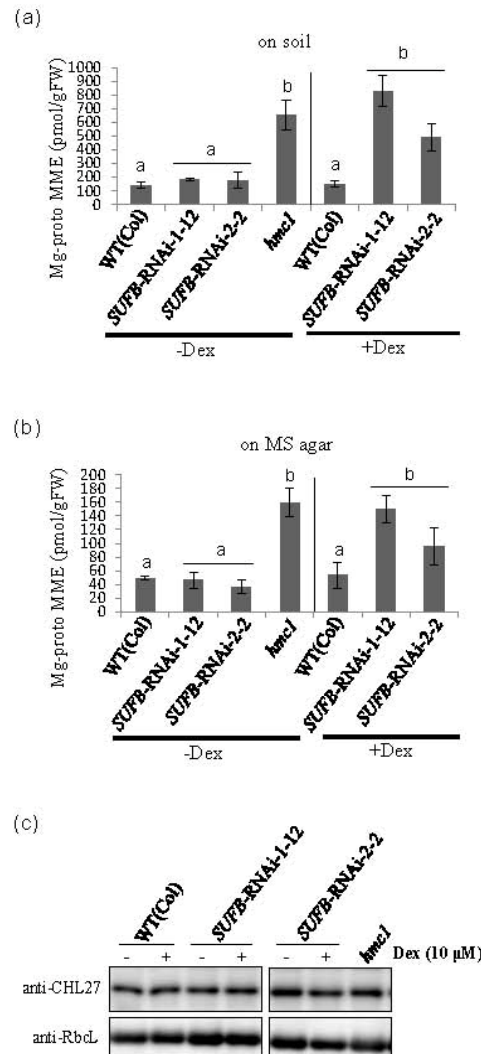


Figure 2. Analysis of chlorophyll biosynthetic intermediates in SUFB-deficient plants. Conditional SUFB-silenced lines (SUFB-RNAi-1-12 and 2-2) were analysed with and without 10 μ M dexamethasone (Dex) together with the SUFB-deficient hmc1 mutant. Mg-proto MME content in (a) developing leaves of 4-week-old plants grown on soil under long-day conditions or (b) in 7-day-old seedlings grown on 1/2 MS medium under long-day conditions. Data points represent the mean \pm SD of four biological replicates. Letters above each bar indicate significant differences ($P < 0.05$) by Tukey's multiple-comparison test. (c) The abundance of Mg-Proto IX cyclase (CHL27) in SUFB-deficient mutant and transgenic lines. Total protein extracts (8 μ g protein) of developing leaves of 4-week-old plants grown on soil under long day conditions were analysed by immunoblotting using anti-CHL27 antisera. Anti-Rubisco large subunit (RbcL) antisera were used to detect RbcL as the loading control.

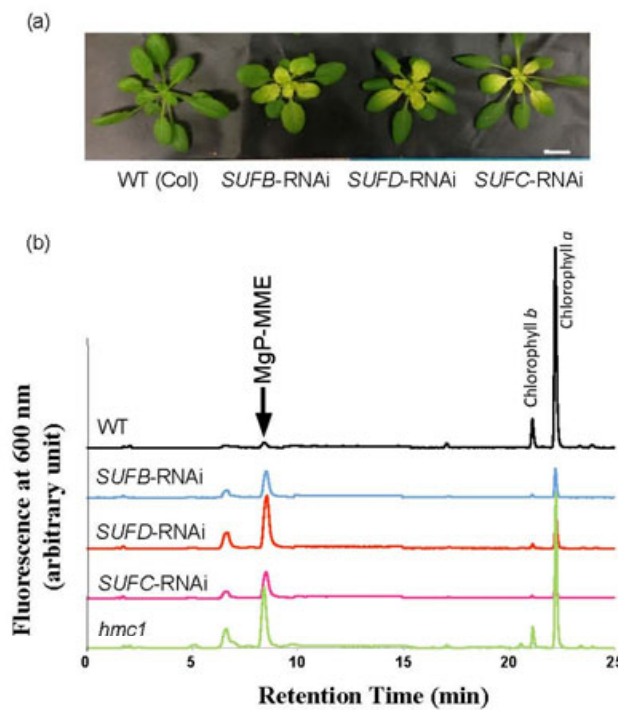


Figure 3. The phenotype of SUFB-, SUFC- and SUFD-deficient plants. Conditional SUFB-, SUFC-, and SUFD-silenced lines were analyzed after 10 μ M dexamethasone (Dex) treatment together with the SUFB-deficient *hmc1* mutant. (a) Phenotype of 4-week-old WT and transgenic plants 7 days after Dex treatment. (b) HPLC profiles of pigments extracted by acetone from young leaves of WT and transgenic plants after Dex treatment. The X axis indicates retention time. The Y axis indicates fluorescence intensity at 600 nm which was excited at 415 nm in arbitrary units.

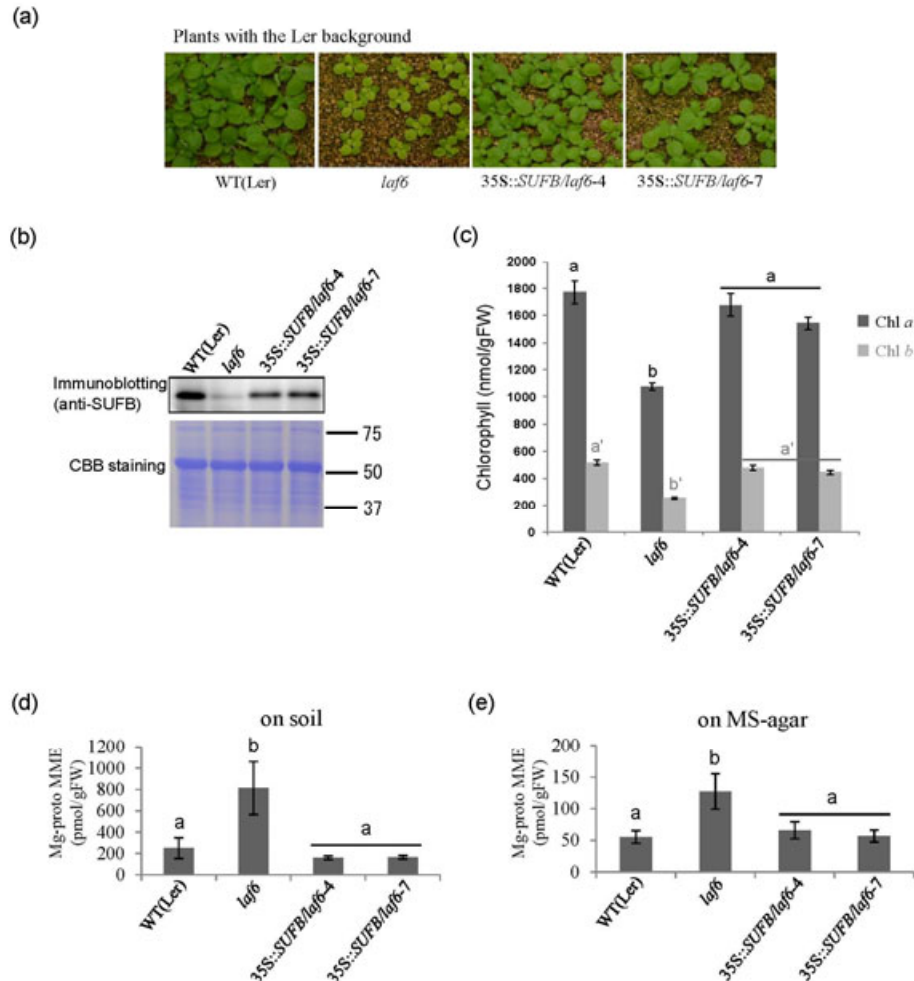


Figure 4. Complementation of laf6 with SUFB. (a) Comparison of laf6 and SUFB overexpressing lines in a laf6 background grown on soil for 3 weeks under long day conditions. (b) SUFB protein levels in the mutant and transgenic lines. Total protein extracts (8 μ g protein) of developing leaves were analyzed by immunoblotting using anti-SUFB antiserum (upper row) and the membrane was subsequently stained by Coomassie brilliant blue (CBB) as a loading control (bottom row). (c) Chlorophyll a and b content of developing leaves of mutant and transgenic plants. (d) Mg-proto MME content in developing leaves of 4-week-old plants grown on soil under long-day conditions. (e) Mg-proto MME content in 7-day-old seedlings grown on 1/2 MS medium under long-day conditions. Data points represent the mean \pm SD of four biological replicates. Letters in black or grey above each bar indicate significant differences ($P < 0.05$) by Tukey's multiple-comparison test.

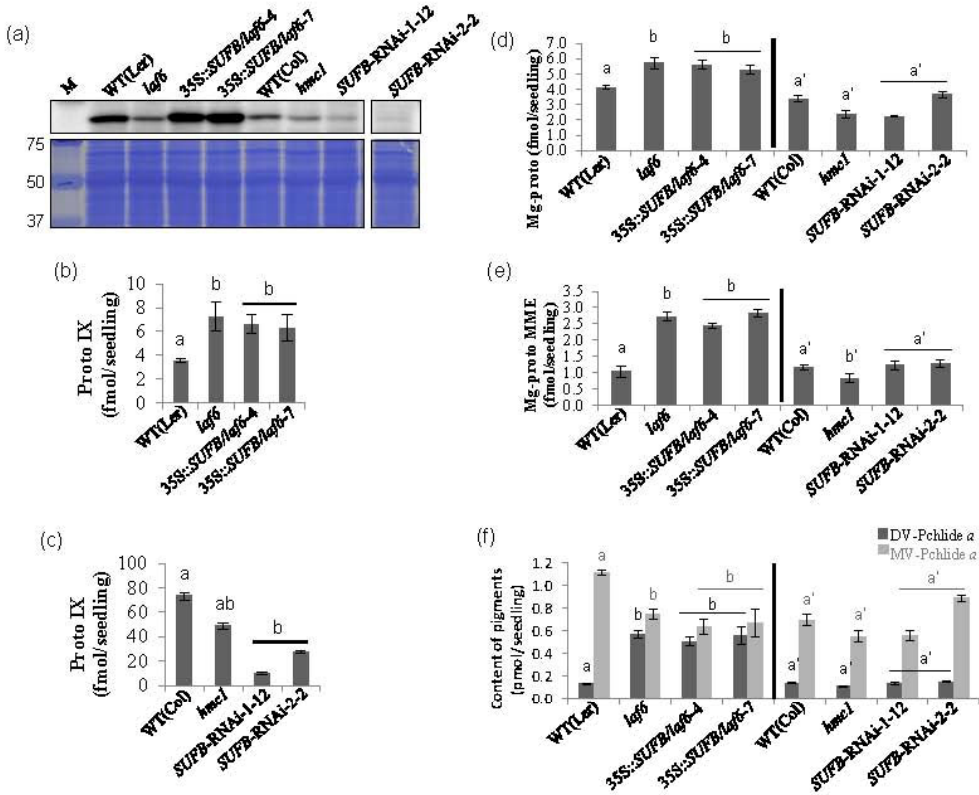


Figure 5. The phenotype of dark-grown SUFB-deficient seedlings. Comparison of 7-day-old etiolated seedlings of conditional SUFB-silenced lines, *hmc1*, *laf6* and *laf6* complemented lines expressing SUFB grown on 1/2 MS medium with 0.8% agar and 1% sucrose. (a) SUFB protein levels in mutant and transgenic seedlings. Total protein extracts (16 μ g protein) were analyzed by immunoblotting using anti-SUFB antiserum (upper row) and the membrane was subsequently stained by Coomassie blue staining as a loading control (lower row). (b), (c) Proto IX contents in etiolated seedlings in the Ler (b) and Col (c) backgrounds. Data points represent the mean \pm SD of three biological replicates. Letters above each bar indicate significant differences ($P < 0.05$) by Tukey's multiple-comparison test. (d) Mg-proto IX and (e) Mg-proto IX-MME contents of mutant and transgenic seedlings. Data points represent the mean \pm SD of three biological replicates. Letters in black (MgP) or in grey (MgP-MME) above each bar indicate significant differences ($P < 0.05$) by Tukey's multiple-comparison test. (f) DV- or MV-Pchlde a contents in mutant and transgenic seedlings. Data points represent the mean \pm SD of four biological replicates. Letters in black (DV-Pchlde a) or in grey (MV-Pchlde a) above each bar indicate significant differences ($P < 0.05$) by Tukey's multiple-comparison test. Proto IX, protoporphyrin IX; MgP, Mg-protoporphyrin IX; MgP-MME, MgP monomethyl ester; DV-Pchlde a, 3,8-divinyl protochlorophylide a; MV-Pchlde a, monovinyl protochlorophylide a.

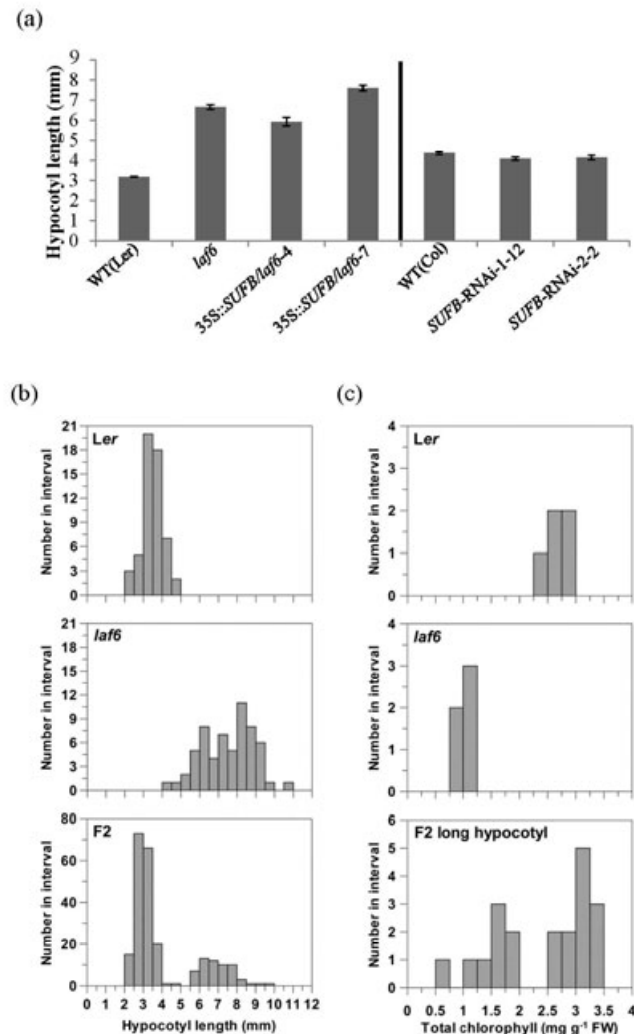


Figure 6. Segregation of the *laf6* long-hypocotyl phenotype. (a) Hypocotyl length of *laf6*, *laf6* expressing SUFB and conditional SUFB-deficient seedling grown for 6 d under far-red (FR) light. Data shown are mean \pm SD of four biological replicates. (b) and (c) Segregation of the long hypocotyl and pale leaf phenotypes of back-crossed *laf6* seedlings. (b) Histogram of hypocotyl lengths of Ler, *laf6* and F2 generation (Ler x *laf6*) seedlings after 6 d growth in FR. (c) Histogram of the foliar chlorophyll content of the parent lines and 20 randomly selected F2 seedlings with long hypocotyls after 6 d FR. Following the FR treatment, all seedlings were supplemented with 3% sucrose and recovered in low intensity white light (WL) (4 d at 5 μ mol m⁻² s⁻¹ followed by 2 d at 25 μ mol m⁻² s⁻¹) before being transferred to WL (100 μ mol m⁻² s⁻¹) for 11 d.